Crystal Structure of an *S*-Formylglutathione Hydrolase from *Pseudoalteromonas haloplanktis* TAC125

Vincenzo Alterio,[1] Vincenzo Aurilia,[2] Alessandra Romanelli,[3] Antonietta Parracino,[2] Michele Saviano,[1] Sabato D'Auria,[2] Giuseppina De Simone[1]

[1] *Istituto di Biostrutture e Bioimmagini-CNR, via Mezzocannone 16, 80134 Napoli, Italy*

[2] *Istituto di Biochimica delle Proteine-CNR, Via Pietro Castellino 111—80131 Napoli, Italy*

[3] *Dipartimento delle Scienze Biologiche, Facoltà di Scienze Biotecnologiche, Università di Napoli Federico II, via Mezzocannone 16, 80134 Napoli, Italy*

Received 8 January 2010; revised 22 February 2010; accepted 22 February 2010
Published online 5 March 2010 in Wiley InterScience (www.interscience.wiley.com). DOI 10.1002/bip.21420

ABSTRACT:

S-*formylglutathione hydrolases (FGHs) constitute a family of ubiquitous enzymes which play a key role in formaldehyde detoxification both in prokaryotes and eukaryotes, catalyzing the hydrolysis of* S-*formylglutathione to formic acid and glutathione. While a large number of functional studies have been reported on these enzymes, few structural studies have so far been carried out. In this article we report on the functional and structural characterization of* Ph*Est, a FGH isolated from the psychrophilic bacterium* Pseudoalteromonas haloplanktis. *According to our functional studies, this enzyme is able to efficiently hydrolyze several thioester substrates with very small acyl moieties. By contrast, the enzyme shows no activity toward substrates with bulky acyl groups. These data are in line with structural studies which highlight for this enzyme a very narrow acyl-binding pocket in a typical* α/β-*hydrolase fold.* Ph*Est represents the first cold-adapted FGH structurally characterized to date; comparison with its mesophilic counterparts of known three-dimensional structure allowed to obtain useful insights into molecular determinants responsible for the ability of this psychrophilic enzyme to work at low temperature.* © *2010 Wiley Periodicals, Inc. Biopolymers 93: 669–677, 2010.*

Keywords: crystal structure; S-formylglutathione hydrolase; psychrophilic organism

This article was originally published online as an accepted preprint. The "Published Online" date corresponds to the preprint version. You can request a copy of the preprint by emailing the Biopolymers editorial office at biopolymers@wiley.com

INTRODUCTION

S-formylglutathione hydrolase (FGH) is an enzyme present both in prokaryotes and eukaryotes, which catalyzes the hydrolysis of *S*-formylglutathione to formic acid and glutathione and constitutes part of a well-conserved formaldehyde detoxification pathway.[1] This enzyme, also known as esterase D, was first purified from human tissues,[2] where polymorphisms in its expression were associated to several diseases including retinoblastoma and Wilson's disease.[3] Subsequently, FGHs were characterized in several organisms such as *Paracoccus denitrificans*,[1] *Saccharomyces cerevisiae*,[4] *Candida boidinii*,[5] *Escherichia coli*,[6,7] and *Arabidopsis thaliana*.[8,9] Regardless of their source, all these enzymes showed remarkable conservation in their sequence and were characterized by the presence of a conserved cysteine residue (generally in position 59), a conserved sequence motif (GHSMGG) containing the catalytic serine, which together with an aspartate and a histidine residue completed a serine hydrolase catalytic triad. Moreover,

Correspondence to: Giuseppina De Simone; e-mail: gdesimon@unina.it

the functional characterization of these enzymes showed that they were not strictly specific to glutathione thioesters, but also showed significant hydrolytic activity against xenobiotic carboxylic esters including methylumbelliferyl acetate.[8,10]

Despite the large number of functional studies reported for this enzyme family, few structural studies are available. In particular, the sole FGHs to be structurally characterized so far are those from *Arabidopsis thaliana* (*At*FGH),[10] *Saccharomyces cerevisiae* (*Sc*FGH),[11] human liver (*h*ESTD),[12] and *Agrobacterium tumefaciens* (*Atu*FGH).[13] Analysis of the structures of these enzymes revealed that, despite the different kingdom of origin, all these proteins share a high degree of structural similarity: they are all dimeric and present a typical α/β-hydrolase fold with the catalytic serine, aspartate, and histidine residues in the canonical positions. These studies also highlighted the role of the aforementioned conserved cysteine residue in regulating enzyme catalytic activity.

We recently identified a new prokaryotic member of the FGH family, hereafter indicated as *Ph*Est, which was isolated from the psychrophilic bacterium *Pseudoalteromonas haloplanktis* TAC125. This 280-residue protein, whose gene corresponds to the ORF PSHAa1385, was originally annotated as a feruloyl esterase, since it hydrolyzed the 4-methylumbelliferyl(p-trimethylammonium cinnamate chloride; MUTMAC), a model substrate for determining feruloyl esterase activity.[14] However, the search for homologues in several genome databases pointed to a high sequence similarity of this enzyme with members of the FGH family, suggesting more appropriate classification as FGH. A preliminary biochemical and functional characterization of this enzyme showed that it has an optimum activity at pH 8.0 and at the temperature of 20°C.[14] Moreover, *Ph*EST can efficiently hydrolyze carboxyl esters such as α-naphtyl-acetate (K_{cat} 2.75 s^{-1}, K_M 0.5 m*M*, k_{cat}/K_M 5.5 s^{-1}/m*M*), β-naphtyl-acetate (K_{cat} 1.8 s^{-1}, K_M 0.5 m*M*, k_{cat}/K_M 3.6 s^{-1}/m*M*), and pNP-acetate (K_{cat} 2 s^{-1}, K_M 0.75 m*M*, k_{cat}/K_M 2.7 s^{-1}/m*M*), while it shows no activity with pNP-esanoate and -dodecanoate as substrates.[14] In view of the wide distribution of FGHs and their role in the formaldehyde detoxification pathway we began to investigate the structure and functions of *Ph*Est. In particular, in this article we describe its crystal structure at 2.20 Å and provide a characterization of the catalytic activity of this enzyme toward several thioester substrates, further supporting the new classification of this enzyme as FGH.

RESULTS

Expression, Purification, and Catalytic Activity of *Ph*Est

The *Ph*Est gene was expressed in *E. coli* strain BL21(DE3) under the control of the T7 RNA polymerase transcription system at 37°C. Five milligrams of purified protein were obtained from 3 g of bacterial cells originated from a 250-ml culture of *E. coli* BL21 (DE3) after IPTG induction and growth for 3 h. The recombinant protein was purified to homogeneity by a single-step Ni^{2+} affinity chromatography as revealed by SDS-PAGE analysis. The protein mass of *Ph*Est was estimated to be 30 kDa by SDS-PAGE, which was consistent with the value predicted from the amino acid sequence. The purified enzyme was also analyzed for its native molecular mass by gel filtration chromatography. It showed a molecular mass of about 60 kDa, suggesting a dimeric structure for this protein.

Enzyme specificity was examined with several thioester substrates, namely p-nitrophenyl-thioacetate (pNP-S-Ac) and three glutathione derivatives: *S*-formylglutathione, *S*-lactoylglutathione, and *S*-acetylglutathione. Thorough analysis of the activity toward pNP-S-Ac was thwarted by the instability of this substrate at concentrations higher than 0.5 m*M*, hampering the calculation of the kinetic parameters. However, a qualitative analysis of enzyme hydrolytic activity revealed that this thioester was hydrolyzed to the same degree as the analogue ester substrate pNP-O-Ac previously investigated.[14] By contrast, analysis of the enzymatic assays with glutathione derivatives showed that *Ph*Est presents quite a high hydrolytic activity toward *S*-acetylglutathione (5.7 U mg^{-1}), while its activity is reduced with *S*-formylglutathione (1.2 U mg^{-1}) and is barely detectable with *S*-lactoylglutathione (4.6×10^{-3} U mg^{-1}).

Overall Structure

*Ph*Est was crystallized in the space group $P2_12_12_1$ with four molecules per asymmetric unit (named A, B, C, and D). Its structure was solved by molecular replacement using the *S. cerevisiae* FGH (PDB code 1PV1) as starting model and refined to a crystallographic *R*-factor of 16.1% and an *R*-free of 20.5% in the 20.00- to 2.20-Å resolution range. The final model consisted of 8660 nonhydrogen atoms, 1054 water molecules, and 4 chloride ions present in the crystallization solution and clearly identified in the Fourier maps. Poor electron density was observed for the N- and C-terminal residue of all the monomers that were not included in the final model. The refined structure presented a good geometry with RMSD from ideal bond lengths and angles of 0.007 Å and 1.4°, respectively. The average temperature factor (*B*) for all atoms was 15.6 $Å^2$. The stereochemical quality of the model was assessed by PROCHECK.[15] The most favored and additionally allowed regions of the Ramachandran plot contained 89.4 and 9.8%, respectively, of the nonglycine residues. Refinement statistics are summarized in Table I.

Table I Data Collection and Refinement Statistics

Crystal parameters	
Space group	$P2_12_12_1$
a (Å)	49.49
B (Å)	129.75
C (Å)	152.67
Number of independent molecules	4
Data collection statistics	
Resolution (Å)	20.00–2.20
Wavelength (Å)	1.54178
Temperature (K)	100
R-sym (%)[a]	5.3 (16.6)
Mean $I/\sigma(I)$	19.5 (5.9)
Total reflections	195285
Unique reflections	49990
Completeness (%)	98.7 (93.6)
Refinement	
Resolution (Å)	20.00–2.20
R-factor (%)[b]	16.1
R-free (%)[b]	20.5
RMSD from ideal geometry:	
Bond lengths (Å)	0.007
Bond angles (°)	1.4
Number of protein atoms	8660
Number of water molecules	1054
Average *B* factor (Å^2):	
All atoms	15.6
Protein atoms	14.3
Water molecules	25.4

Values in parentheses refer to the highest resolution shell (2.28–2.20 Å).

[a] $R_{sym} = \Sigma|I_i - <I>|/\Sigma I_i$; over all reflections.

[b] $R_{factor} = \Sigma||F_o| - |F_c||/\Sigma|F_o|$; R_{free} calculated with 5% of data withheld from refinement.

*Ph*Est is a compact globular protein, whose roughly ellipsoidal shape is ~40 × 40 × 50 Å^3 in size. Its structure shows the typical features of the α/β-hydrolase fold: it consists of a central nine-stranded mixed β-sheet surrounded by nine α-helices, four 3_{10}-helices, and one π-helix (Figures 1A and 1B). In agreement with gel filtration analysis the four independent molecules in the asymmetric unit form two dimers very similar to those observed for the other FGHs with known crystal structure.[10–13] Within each dimer, the two monomers interact via eight hydrogen bonds (Table II) and numerous van der Waals interactions, thus generating an interface area that extends over 1754 Å^2. The two active sites stand opposite to each other and are perfectly accessible to the substrate (see Figure 2).

The four molecules in the asymmetric unit are almost identical: superimposition carried out on the Cα positions of all 278 residues leads to an RMSD ranging from 0.17 to 0.22 Å. Therefore, the following discussion will be conducted based on only one arbitrarily chosen monomer, unless otherwise stated.

Catalytic Triad and Binding Pockets

*Ph*Est contains a catalytic triad formed by residues Ser147, Asp225, and His258, all located according to the classic arrangement characterizing the α/β-hydrolases. Ser147 is part of the hexapeptide sequence Gly-His-Ser-Met-Gly-Gly, conserved in all characterized FGHs. It is located at the apex of a sharp turn, called nucleophilic elbow, which connects strand β6 and the following helix α5 (Figure 1A). The sharpness of the turn causes a strained conformation of the catalytic serine with backbone ϕ and ψ angles lying in an unfavorable region of the Ramachandran plot (ϕ = 55.9° and ψ = −110.0°). A hydrogen bond interaction between Ser147OG and His258NE2 atoms contributes to the stabilization of this conformation (see Figure 3). The active site histidine is located in a five-residue loop connecting strand β9 to helix α9 (Figures 1A and 1B). It is hydrogen bonded to the third residue of the catalytic triad, Asp225 (His258ND1—Asp225OD2 = 2.63 Å), which in turn interacts with Phe227 (Asp225OD2—-Phe227N = 2.79 Å) and Gln221 (Asp225OD2—Gln221NE2 = 3.13 Å; see Figure 3). As already observed for *At*FGH,[10] *Sc*FGH,[11] *h*ESTD,[12] and *Atu*FGH,[13] Leu54 and Met148 complete the catalytic machinery, with their main chain NH groups being used to define the oxyanion hole, required for the oxyanion intermediate stabilization during the catalytic process. In fact, the nitrogen backbone atoms of these residues are hydrogen bonded to a water molecule that approximately mimics the position occupied by the negatively charged oxygen of the tetrahedral intermediate arising from the nucleophilic attack of the catalytic serine on the ester substrate (see Figure 3).

Detailed inspection of the solvent accessible surface reveals the presence of a large cleft, delimited by residues Thr55, Cys56, Asn60, Lys64, His258, Ser259, and Tyr260, that spans from the protein surface to the catalytic serine. By contrast, a very small cavity, bordered by residues Leu54, Ile173, Trp181, Phe227, and Leu232 is located close to this catalytic serine. The structural superposition of *Ph*Est with other esterases in complex with substrate analogues[17,18] allowed the cavity to be identified as the acyl binding pocket and the cleft as the alcohol/thiol binding pocket of the ester substrate. Interestingly, as already observed for other FGHs whose three dimensional structure has been solved, the acyl binding pocket is very small and allows for the accommodation of substrates with very short acyl chains, like formyl- or acetyl-esters. Instead, the alcohol/thiol binding pocket is very large and allows for the accommodation of very large moieties, thus explaining the high activity of this enzyme toward esters of glutathione and umbelliferon. Cys56, the highly conserved

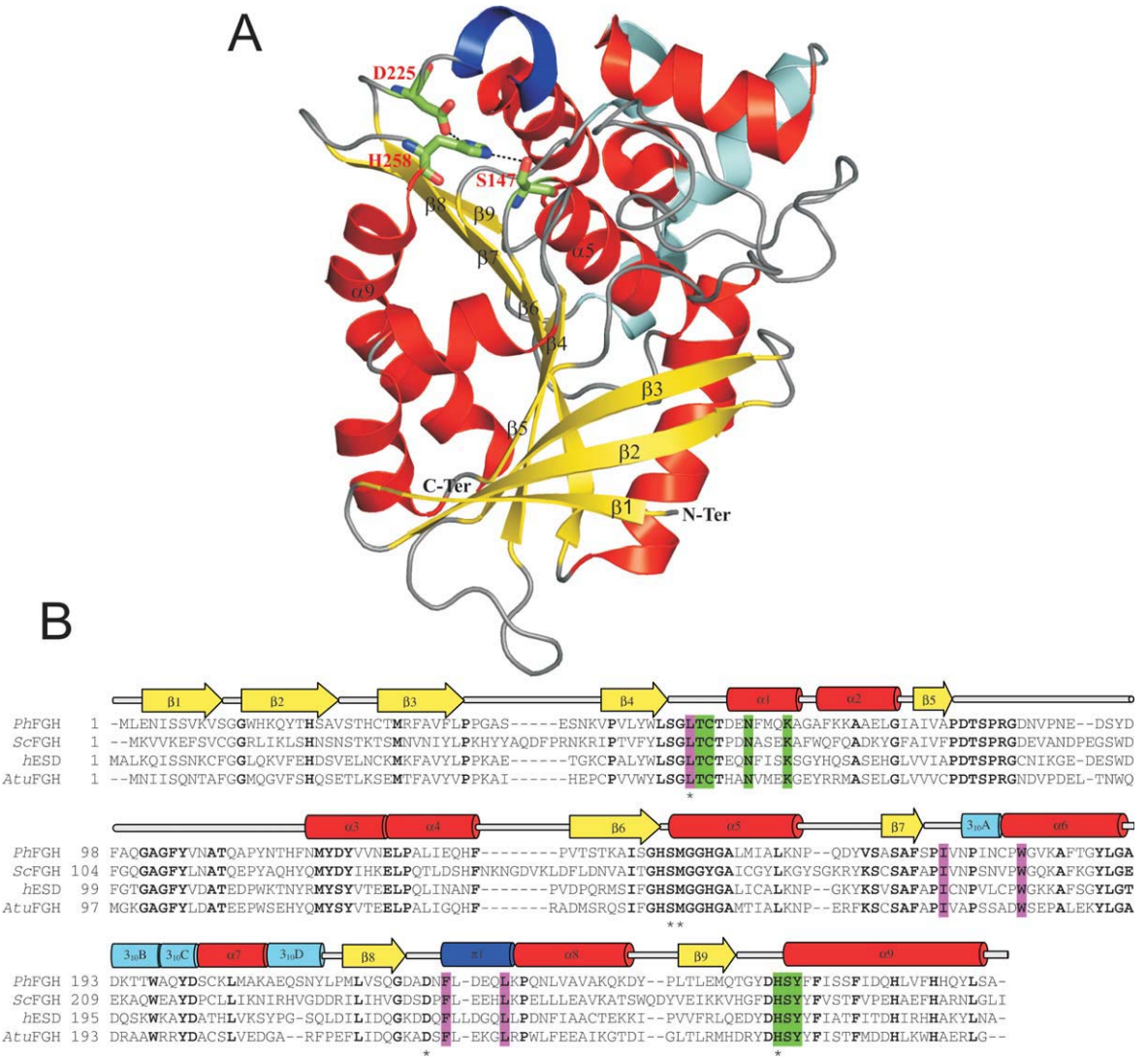

FIGURE 1 (**A**) *Ph*Est overall fold. *β*-strands are reported in yellow (*β*1, 3–10; *β*2, 13–22; *β*3, 27–35; *β*4, 45–51; *β*5, 77–80; *β*6, 137–145; *β*7, 167–170; *β*8, 217–222; *β*9, 248–253), α-helices in red (α1, 58–65; α2, 67–75; α3, 118–125; α4, 125–135; α5, 147–160; α6, 179–191; α7, 201–208; α8, 233–245; α9, 259–279), 3_{10}-helices in cyan (3_{10}A, 175–178; 3_{10}B, 193–197; 3_{10}C, 197–200; 3_{10}D, 210–214) and *π*-helices in blue (*π*1, 227–232). Secondary structure assignments were obtained from PROMOTIF.[16] (**B**) Structure-based sequence alignment of *Ph*Est with *Sc*FGH (PDB code 1PV1),[11] *h*ESTD (PDB code 3FCX)[12] and *Atu*FGH (PDB code 3E4D).[13] Secondary structural elements refer to *Ph*Est. Catalytic triad and oxyanion hole residues are starred, strictly conserved residues are bold while residues delimiting the acyl and alcohol/thiol binding pockets are highlighted in magenta and green, respectively.

residue that is assumed to play a key role into FGH regulation,[10,11] is located on the edge of the alcohol/thiol binding site in the loop connecting strand *β*4 to helix α1, at ∼9 Å from Ser147 (SerCB-CysCB = 8.84 Å).

Structural Comparison with Other FGHs

*At*FGH,[10] *Sc*FGH,[11] *h*ESTD,[12] and *Atu*FGH[13] are the only examples of proteins belonging to the FGH family to be structurally characterized to date. However, since the PDB coordinate file of *At*FGH is not available in the PDB database, this enzyme will not be used in the structural comparisons below. Despite the difference in the kingdom of origin, *Ph*Est, *Sc*FGH, *h*ESTD, and *Atu*FGH present a high sequence identity (42% for *Ph*Est/*Sc*FGH, 52% for *Ph*Est/*h*ESTD, and 52% for *Ph*Est/*Atu*FGH) and a substantial degree of three-dimensional similarity. Indeed, the RMSD for the superposition of the backbone atoms of *Ph*Est with the corresponding atoms in *Sc*FGH,[11] *h*ESTD,[12] and *Atu*FGH[13] was calculated

Table II Intermolecular Hydrogen Bonds Stabilizing the Dimeric Structure of *Ph*Est

Chain A	Chain B	Distance (Å)
Lys9NZ	Thr254O	2.82
Ser11N	Ser265OG	2.78
Lys69NZ	Asp268OD2	2.84
Tyr256OH	Gly12N	2.67
Gly12N	Tyr256OH	2.92
Thr254O	Lys9NZ	2.95
Asp268OD2	Lys69NZ	3.02
Ser265OG	Ser11N	2.96

as 1.3, 1.1, and 1.0 Å, respectively. The main differences were observed in the loops connecting β3 and β4, β5 and α3, α4 and β6, and α8 and β9, where several insertions or deletions were observed in *Ph*Est with respect to the other enzymes (Figure 1B). Since these regions are located far away from the active site, the observed differences should not influence either catalytic activity or substrate binding. The active site regions of the three enzymes were almost superimposable. Interestingly, sequence alignment reported in Figure 1B revealed that the structural similarity in this region was also associated to a total conservation of the amino acids delimiting the acyl and alcohol/thiol binding pockets.

Structural Determinants of Cold Adaptation

Psychrophilic or cold-adapted enzymes have two main properties: rapid inactivation at moderately high temperature and a high specific activity at low temperatures. Much research effort has been made in recent years to obtain information on the molecular determinants responsible for these properties by comparing both sequences and three-dimensional structures of psycrophilic enzymes with their mesophilic counterparts. From sequence analysis a decreased number of proline residues, an increased number of glycine residues, fewer arginine residues, and a lower arginine/(arginine + lysine) ratio have emerged as a hallmark of psycrophilic enzymes.[19–21] The sequence comparison of *Ph*Est with its mesophilic counterparts *Sc*FGH,[11] *h*ESTD,[12] and *Atu*FGH[13] reveals that among these factors only the number of arginine residues and the value of the arginine/(arginine + lysine) ratio show a clear correlation with enzyme psychrophilicity (see Table III).

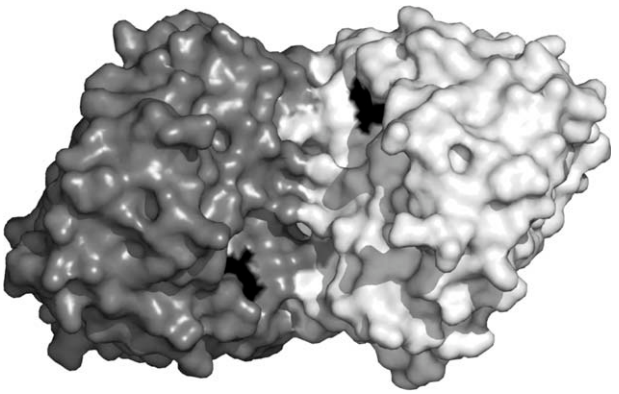

FIGURE 2 Dimeric structure of *Ph*Est with one monomer colored white, the other gray. The active site cavity of each monomer is reported in black.

On the other hand, structural comparisons have shown that several factors, such as a reduced number of salt bridges and hydrogen bonds,[25,26] a reduced contribution of charged residues to the accessible and buried surface,[27,28] and an increased contribution of hydrophobic residues to the surface area[26] can influence the ability of cold-adapted enzymes to work at low temperature. Thus, all these parameters were compared between *Ph*EST and its mesophilic counterparts and reported in Table III. Close analysis of this table reveals that among the considered parameters the number of ionic interactions calculated at 4 and 6 Å displayed the clearest correlation with enzyme psychrophilicity. Indeed, *Ph*Est shows the fewest ion pairs within the structures analyzed, indicating that the enzyme most likely adopts this strategy to maintain appropriate protein flexibility at low temperature. The amino

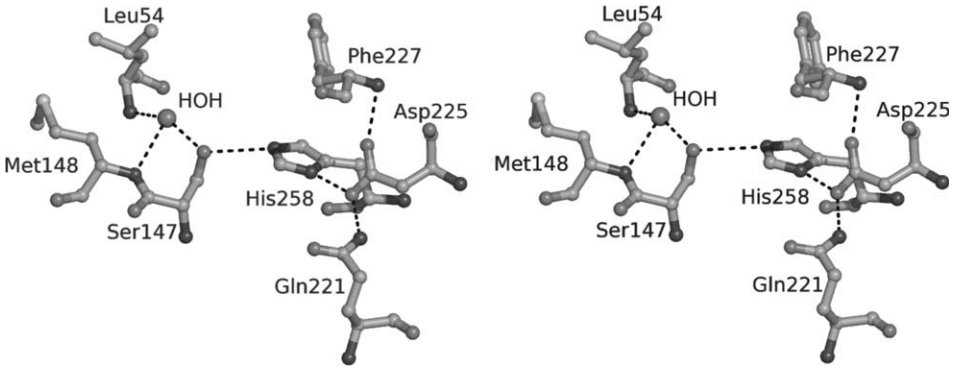

FIGURE 3 Stereo view of the *Ph*Est active site. Hydrogen bonds are shown as dotted lines.

Table III Comparison of Sequences and Structural Features of *Ph*Est, *Sc*FGH, *h*ESD, and *Atu*FGH

	*Ph*Est	*Sc*FGH	*h*ESD	*Atu*FGH
Sequence comparison				
Number of Arg residues	2 (0.7)[a]	8 (2.7)[a]	5 (1.8)[a]	14 (5.0)[a]
Number of Lys residues	15 (5.4)[a]	22 (7.4)[a]	22 (7.8)[a]	11 (4.0)[a]
Arg/(Arg + Lys)	0.11	0.27	0.19	0.56
Number of Gly residues	18 (6.4)[a]	24 (8.0)[a]	22 (7.8)[a]	23 (8.3)[a]
Number of Pro residues	16 (5.7)[a]	16 (5.4)[a]	16 (5.7)[a]	15 (5.4)[a]
Number of Gln + Asn residues	30 (10.8)[a]	26 (8.7)[a]	23 (8.2)[a]	14 (5.1)[a]
Structural comparison				
Number of ion pairs (4 Å)[b]	5 (0.018)[c]	12 (0.040)[c]	8 (0.028)[c]	17 (0.061)[c]
Number of ion pairs (6 Å)[b]	15 (0.054)[c]	24 (0.080)[c]	20 (0.071)[c]	29 (0.104)[c]
Number of hydrogen bonds[d]	158 (0.56)[e]	156 (0.52)[e]	157 (0.56)[e]	159 (0.57)[e]
Total solvent accessible surface area ($Å^2$)[f]	20636	23168	20790	20476
>Charged residues[f]	7180 (34.8)[g]	11573 (50.0)[g]	8742 (42.0)[g]	10784 (52.7)[g]
>Polar residues[f]	8795 (42.6)[g]	6234 (26.9)[g]	6152 (29.6)[g]	4560 (22.3)[g]
>Hydrophobic residues[f]	4661 (22.6)[g]	5361 (23.1)[g]	5897 (28.4)[g]	5132 (25.0)[g]
Gln contribution to the surface area ($Å^2$)[f]	2371 (11.5)[g]	1312 (5.7)[g]	1552 (7.5)[g]	942 (4.6)[g]
Asn contribution to the surface area ($Å^2$)[f]	1968 (9.5)[g]	1887 (8.1)[g]	1320 (6.3)[g]	761 (3.7)[g]
Gln + Asn contribution to the surface area ($Å^2$)[f]	4338 (21.0)[g]	3198 (13.8)[g]	2872 (13.8)[g]	1703 (8.3)[g]

[a] Percentage respect to the total number of protein residues.

[b] Salt bridges within a distance of 4 and 6 Å, measured on the chain A of each enzyme, using the program PIC (http://crick.mbu.iisc.ernet.in/~PIC/index.html).[22]

[c] Ion pairs normalized respect to the number of protein residues.

[d] Intramolecular hydrogen bonds counted on chain A of each structure, using the program CNS,[23] a maximum distance between acceptor oxygen and donor nitrogen of 3.5 Å and a minimum angle between acceptor carbon, acceptor oxygen and donor nitrogen of 120°.

[e] Hydrogen bonds normalized respect to the number of protein residues.

[f] Surface areas calculated using the program GRASP[24] with a 1.4 Å probe and taking into account the physiological dimer of each structure. The amino acid residues were grouped as follows: charged (R,K,D,E,H), polar (S,T,Q,N,Y), hydrophobic (G,A,L,I,W,P,F,M,C,V).

[g] Percentage of surface respect to the total solvent accessible area.

acid composition of the protein surface is another major feature that distinguishes *Ph*Est from the other three enzymes. In particular, in agreement with literature data, *Ph*Est shows the smallest portion of charged surface area, while no agreement with the literature data is observed for the hydrophobic surface area, since *Ph*Est presents a lower or approximately equal content of hydrophobic amino acids on its molecular surface. Interestingly, a large amount of *Ph*Est surface is made of polar residues. The presence of polar amino acids on the surface of cold-adapted enzymes is considered an extremely important factor for proper protein solvation and for maintaining the right molecular flexibility, due to the high viscosity and high surface tension of water at low temperatures.[29] It is worth noting that the *Ph*Est polar surface area has a higher asparagine and glutamine content, which compensates for the reduction in surface charged residues. A relative abundance of these amino acids is typical in psychrophilic organisms and has been observed in the whole genome of *Pseudoalteromonas haloplanktis* TAC125.[30] This trend provides evidence for the adaptation of the bacterium to its cold environment. Indeed, glutamine and asparagine side chains are heat-labile and are predisposed to deamination at high temperatures,[31] while are quite stable in a cold environment, thus explaining their increased content in cold-adapted proteins.[32]

DISCUSSION

Formaldehyde is a very reactive compound that has been classified as a potential human carcinogen. It is a widespread pollutant as well as a common by-product of primary metabolism originated by the spontaneous dissociation of 5,10-methylene tetrahydrofolate and by protein-repair and oxidative-demethylation reactions.[33] To perform the detoxification from formaldehyde, different organisms have developed different systems.[34–36] However, the glutathione-dependent repair system is the most widespread in nature, being found in most prokaryotes and all eukaryotes.[1,33,37,38] In this process formaldehyde reacts with reduced glutathione (GSH) to yield *S*-hydroxymethylglutathione, which is subsequently oxidized by NAD-dependent formaldehyde dehydrogenase (FALDH) to *S*-formylglutathione. Lastly, this compound is hydrolyzed to formate and GSH by *S*-formylglutathione hydrolase (FGH). Thus both FALDH and FGH are part of a GSH-dependent formaldehyde

oxidation pathway. However, while FALDH was extensively characterized in recent years both structurally and biochemically,[39–42] FGH has received much less attention.

In this article we reported the characterization of the catalytic activity and crystallographic structure of *Ph*Est, a FGH isolated from the psychrophilic bacterium *Pseudoalteromonas haloplanktis* TAC125. The kinetic characterization of the enzyme with several thioester substrates demonstrated that *Ph*EST can efficiently hydrolyze substrates with small acyl moieties such as p-nitrophenyl-*S*-acetate, *S*-acetylglutathione, and *S*-formylglutathione, while it shows no activity toward substrates with a bulky acyl group such as *S*-lactoylglutathione. Analysis of the crystallographic structure correlates well with these findings. Indeed, the enzyme, which shows a typical α/β-hydrolase fold, is characterized by the presence of a very small acyl binding pocket and a large alcohol/thiol binding pocket. These observations are also in line with previously reported kinetic studies on this enzyme, which showed that it can hydrolyze with high efficiency α-naphtyl-, β-naphtyl, and pNP-acetate esters, whilst showing no activity with pNP-esanoate and -dodecanoate.[14] Interestingly, the structural comparison of *Ph*EST with all other FGHs with known three dimensional structure[11–13] reveals that, irrespective of their source, these enzymes show a remarkable degree of three dimensional similarities and, more surprisingly, a complete conservation of all residues delimiting the acyl and alcohol/thiol binding pockets (see Figure 1B). These findings go some way to explaining the strong similarity in substrate specificity exhibited by these enzymes and further support the idea, already suggested by several authors,[1,7–9] that the FGH enzyme is part of an universal detoxification pathway shared by a variety of organisms.

*Ph*Est is the first cold-adapted FGH to be structurally characterized. In recent years, many research groups have focused on cold-adapted enzymes since the peculiar features of these proteins make them particularly interesting for applications in industrial processes.[43] Indeed, their high catalytic efficiency at low temperature together with their rapid inactivation at temperature as low as 30°C confer great potential on these enzymes in biotechnological applications. For the above reasons, identification of the molecular basis of the cold adaptation for different enzyme families is of great topical interest. The availability of structural data for *Ph*Est and its mesophilic analogues *Sc*FGH, *h*ESTD, and *Atu*FGH provided the opportunity to identify subtle structural differences which may account for their ability to cope with different environmental temperatures. In particular, a reduced number of ionic interactions together with a decreased value of the charged surface area seem to have a major role in the capability of the psychrophilic enzyme under investigation to work at low temperature. Other cold adaptations are not evident, further supporting the idea that each enzyme family can choose a different strategy for dealing with low environmental temperature.

In conclusion our structural studies of *Ph*Est obtained further insights into the catalytic and structural features of FGH*s* and identified some possible molecular determinants of cold adaptation in this enzyme family; however, further mutagenesis studies are necessary to test these hypotheses.

MATERIALS AND METHODS

Protein Expression and Purification

The gene *Ph*Est, encoded by the ORF PSHAa 1385, was cloned into the expression vector pET28a in frame, at its N-terminus, with a six-histidine stretch.[14] N-terminus His6-S-tagged protein from pET28a construct was overexpressed following transformation in *E. coli* BL21(DE3). After growth at 37°C on Luria-Bertani medium supplemented with 50 μg of kanamycin ml^{-1}, the cells were recovered and lysed by sonication (Soniprep; Sanyo). Induction was carried out by adding 0.1 m*M* IPTG to a culture at an optical density of 0.5 measured at 600 nm, and then incubating the culture at 37°C for 3 h. The obtained protein was purified by nickel affinity chromatography as described by the manufacturer (Novagen). Thrombin cutting on column was used to obtain the protein without the His stretch at its N-terminal. The purified protein was analyzed by SDS-PAGE as described by Laemmli[44] and by Western Blotting with anti-His antibodies.

Synthesis of Thioesters

S-lactoylglutathione and *p*-nitrophenyl-thioacetate were provided by Sigma-Aldrich, while *S*-acetylglutathione and *S*-formylglutathione were synthesized following procedures reported elsewhere.[45] Products were purified by HPLC on a Phenomex Jupiter 10μ Proteo 90Å 250 × 10.00 mm^2 column, and analyzed by LC-MS on a Thermo Finnigan (MSQ) instrument with a Phenomenex Jupiter 10μ Proteo 90Å 250 × 10.00 mm^2 column. *S*-acetylglutathione was purified using a gradient of acetonitrile (0.1% TFA) in water (0.1% TFA) from 0 to 40% in 45 min (Mass: calculated: 349.4 Da; observed 349.9 Da). *S*-formylglutathione was purified using an isocratic gradient of water (0.1% TFA) of 45 min (Mass: calculated: 335.1 Da; observed 335.4 Da)

Enzymatic Assays

Protein concentration was determined as described by Bradford,[46] using the BioRad protein staining assay, and BSA as standard. Thioesterase activity was determined at 20°C by using pNP-O-Ac and pNP-S-Ac as substrates. The assays were performed in 1 ml of 20 m*M* sodium phosphate buffer pH 7.4 containing 5 m*M* pNP-O-Ac and 0.5 m*M* pNP-S-Ac. The release of p-nitrophenol was continuously monitored at 405 nm by a Cary ultraviolet-visible spectrophotometer equipped with a Dual Cell Peltier Temperature Controller (Varian). One enzyme unit was defined as the amount of enzyme releasing 1 μmol of p-nitrophenol per minute under the described conditions. The assays with glutathione thioesters (*S*-formylglutathione, *S*-lactoylglutathione, and *S*-acetylglutathione) at a concen-

tration of 1 m*M* were carried out at 20°C in 20 m*M* sodium phosphate buffer pH 7.4. The hydrolysis of S-derivatives of glutathione was determined by monitoring the respective decrease in absorbance at 240 nm.

Crystallization and X-Ray Data Collection

*Ph*Est was crystallized at 293 K using the hanging drop vapor diffusion technique. Drops were prepared by mixing 1 μl of enzyme solution (4 mg ml^{-1} in 25 m*M* TRIS-HCl, pH 7.3) with 1 μl of precipitant solution (20% (w/v) PEG MME 5000, 0.2*M* sodium acetate, 0.1*M* TRIS-HCl, pH 7.0), and equilibrated over a well containing 1 ml of precipitant solution. Crystals appeared after 3 days and grew in about one week to maximum dimensions of 0.3 × 0.2 × 0.2 mm^3. A complete dataset was collected at 2.20-Å resolution from a single crystal at the temperature of 100 K, with a copper rotating anode generator developed by Rigaku and equipped with Rigaku Saturn CCD detector. Prior to cryogenic freezing, crystals were transferred to the precipitant solution with the addition of 15% (w/v) glycerol. Data were processed using the HKL2000 crystallographic data resolution package (Denzo/Scalepack).[47] The crystals belonged to the space group $P2_12_12_1$ with unit cell dimensions of a = 49.49 Å, b = 129.75 Å, c = 152.67 Å. The Matthews coefficient (V_M = 1.99 Å^3 Da^{-1}) indicated that the crystallographic asymmetric unit contained four molecules according to a solvent content of 38%. Data collection statistics are reported in Table I.

Structure Determination and Refinement

The structure of *Ph*Est was solved by molecular replacement technique using the program AMoRe[48] and the crystallographic structure of the *Sc*FGH (PDB code 1PV1)[11] as model template. The rotation and translation functions were calculated using data between 15.0 and 3.5 Å resolution. The one-body translation search, using the centred-overlap function (c-o), on the first 50 rotation solutions led to a single solution with a correlation coefficient of 25.4% and an *R*-factor of 52.1%. The n-body translation search carried out with the phased-translation function (p-t), by including a PC refinement before each n-body translation search led to finding the remaining three molecules contained into the asymmetric unit. This improved the correlation coefficient and the *R*-factor to 73.8 and 32.7%, respectively. Refinement of the structure was carried out using CNS[23] and model building was performed with O.[49] The first cycles of the refinement were carried out with four-fold NCS-restraints with an energy barrier of 300 kcal mol^{-1} Å^2. After *R*-factor and *R*-free reached 21.7 and 24.1%, respectively, the NCS restraints were removed, and further cycles of manual rebuilding and positional and temperature factor refinement were necessary to reduce the crystallographic *R*-factor and *R*-free values (in the 20.00- to 2.20-Å resolution range) to 16.1 and 20.5%, respectively. Data refinement statistics are summarized in Table I. Coordinates and structure factors were deposited in the Protein Data Bank (accession code 3LS2).

REFERENCES

1. Harms, N.; Ras, J.; Reijnders, W. N.; van Spanning, R. J.; Stouthamer, A. H. J Bacteriol 1996, 178, 6296–6299.
2. Uotila, L.; Koivusalo, M. J Biol Chem 1974, 249, 7664–7672.
3. Lee, E. Y.; Lee, W. H. Proc Natl Acad Sci USA 1986, 83, 6337–6341.
4. Degrassi, G.; Uotila, L.; Klima, R.; Venturi, V. Appl Environ Microbiol 1999, 65, 3470–3472.
5. Yurimoto, H.; Lee, B.; Yano, T.; Sakai, Y.; Kato, N. Microbiology 2003, 149, 1971–1979.
6. Herring, C. D.; Blattner, F. R. J Bacteriol 2004, 186, 6714–6720.
7. Gonzales, C. F.; Proudfoot, M.; Brown, G.; Korniyenko, Y.; Mori, H.; Savchenko, A. V.; Yakunin, A. F. J Biol Chem 2006, 281, 14514–14522.
8. Kordic, S.; Cummins, I.; Edwards, R. Arch Biochem Biophys 2002, 399, 232–238.
9. Haslam, R.; Rust, S.; Pallett, K.; Cole, D.; Coleman, J. Plant Physiol Biochem 2002, 40, 281–288.
10. Cummins, I.; McAuley, K. M.; Fordham-Skelton, A.; Schwoerer, R.; Steel, P. G.; Davis, B. G.; Edwards, R. J Mol Biol 2006, 359, 422–432.
11. Legler, P. M.; Kumaran, D.; Swaminathan, S.; Studier, F. W.; Millard, C. B. Biochemistry 2008, 47, 9592–9601.
12. Wu, D.; Li, Y.; Song, G.; Zhang, D.; Shaw, N.; Liu, Z. J. FASEB J 2009, 23, 1441–1446.
13. van Straaten, K. E.; Gonzalez, C. F.; Valladares, R. B.; Xu, X.; Savchenko, A. V.; Sanders, D. A. Protein Sci 2009, 18, 2196–2202.
14. Aurilia, V.; Parracino, A.; Saviano, M.; Rossi, M.; D'Auria, S. Gene 2007, 397, 51–57.
15. Laskowsky, R. A.; MacArthur, M. W.; Moss, D. S.; Thornton, J. M. J Appl Cryst 1993, 26, 283–291.
16. Hutchinson, E. G.; Thornton, J. M. Protein Sci 1996, 5, 212–220.
17. De Simone, G.; Galdiero, S.; Manco, G.; Lang, D.; Rossi, M.; Pedone, C. J Mol Biol 2000, 303, 761–771.
18. De Simone, G.; Mandrich, L.; Menchise, V.; Giordano, V.; Febbraio, F.; Rossi, M.; Pedone, C.; Manco, G. J Biol Chem 2004, 279, 6815–6823.
19. Bentahir, M.; Feller, G.; Aittaleb, M.; Lamotte-Brasseur, J.; Himri, T.; Chessa, J. P.; Gerday, C. J Biol Chem 2000, 275, 11147–11153.
20. Hoyoux, A.; Jennes, I.; Dubois, P.; Genicot, S.; Dubail, F.; François, J. M.; Baise, E.; Feller, G.; Gerday, C. Appl Environ Microbiol 2001, 67, 1529–1535.
21. Lonhienne, T.; Zoidakis, J.; Vorgias, C. E.; Feller, G.; Gerday, C.; Bouriotis, V. J Mol Biol 2001, 310, 291–297.
22. Tina, K. G.; Bhadra, R.; Srinivasan, N. Nucleic Acids Res 2007, 35, W473–W476.
23. Brünger, A. T.; Adams, P. D.; Clore, G. M.; De Lano, W. L.; Gros, P.; Grosse-Kunstleve, R. W.; Jiang, J. S.; Kuszewski, J.; Nilges, M.; Pannu, N. S.; Read, R. J.; Rice, L. M.; Simonson, T.; Warren, G. L. Acta Crystallogr Sect D 1998, 54, 905–921.
24. Nicholls, A.; Sharp, K. A.; Honig, B. Proteins 1991, 11, 281–296.
25. Feller, G.; Arpigny, J. L.; Nminx, E.; Geday, C. Camp Biochem Physiol 1997, 118A, 495–499.
26. Siddiqui, K. S.; Cavicchioli, R. Annu Rev Biochem 2006, 75, 403–433.
27. Saunders, N. F.; Thomas, T.; Curmi, P. M.; Mattick, J. S.; Kuczek, E.; Slade, R.; Davis, J.; Franzmann, P. D.; Boone, D.; Rusterholtz, K.; Feldman, R.; Gates, C.; Bench, S.; Sowers, K.; Kadner, K.; Aerts, A.; Dehal, P.; Detter, C.; Glavina, T.; Lucas, S.; Richardson, P.; Larimer, F.; Hauser, L.; Land, M.; Cavicchioli, R. Genome Res 2003, 13, 1580–1588.

28. Methé, B. A.; Nelson, K. E.; Deming, J. W.; Momen, B.; Melamud, E.; Zhang, X.; Moult, J.; Madupu, R.; Nelson, W. C.; Dodson, R. J.; Brinkac, L. M.; Daugherty, S. C.; Durkin, A. S.; DeBoy, R. T.; Kolonay, J. F.; Sullivan, S. A.; Zhou, L.; Davidsen, T. M.; Wu, M.; Huston, A. L.; Lewis, M.; Weaver, B.; Weidman, J. F.; Khouri, H.; Utterback, T. R.; Feldblyum, T. V.; Fraser, C. M. Proc Natl Acad Sci USA 2005, 102, 10913–10918.
29. Kumar, S.; Nussinov, R. ChemBioChem 2004, 5, 280–290.
30. Médigue, C.; Krin, E.; Pascal, G.; Barbe, V.; Bernsel, A.; Bertin, P. N.; Cheung, F.; Cruveiller, S.; D'Amico, S.; Duilio, A.; Fang, G.; Feller, G.; Ho, C.; Mangenot, S.; Marino, G.; Nilsson, J.; Parrilli, E.; Rocha, E. P.; Rouy, Z.; Sekowska, A.; Tutino, M. L.; Vallenet, D.; von Heijne, G.; Danchin, A. Genome Res 2005, 15, 1325–1335.
31. Lee, D. Y.; Kim, K. A.; Yu, Y. G.; Kim, K. S. Biochem Biophys Res Commun 2004, 320, 900–906.
32. Bauvois, C.; Jacquamet, L.; Huston, A. L.; Borel, F.; Feller, G.; Ferrer, J. L. J Biol Chem 2008, 283, 23315–23325.
33. Hanson, A. D.; Gage, D. A.; Shachar-Hill, Y. Trends Plant Sci 2000, 5, 206–213.
34. Bystrykh, L. V.; Govorukhina, N. I.; Van Ophem, P. W.; Hektor, H. J.; Dijkhuizen, L.; Duine, J. A. J Gen Microbiol 1993, 139, 1979–1985.
35. Sakai, Y.; Murdanoto, A. P.; Sembiring, L.; Tani, Y.; Kato, N. FEMS Microbiol Lett 1995, 127, 229–234.
36. Ito, K.; Takahashi, M.; Yoshimoto, T.; Tsuru, D. J Bacteriol 1994, 176, 2483–2491.
37. Uotila, L.; Koivusalo, M. Arch Biochem Biophys 1979, 196, 33–45.
38. Lee, W. H.; Wheatley, W.; Benedict, W. F.; Huang, C. M.; Lee, E. Y. Proc Natl Acad Sci USA 1986, 83, 6790–6794.
39. Moulis, J. M.; Holmquist, B.; Vallee, B. L. Biochemistry 1991, 30, 5743–5749.
40. Jensen, D. E.; Belka, G. K.; Du Bois, G. C. Biochem J 1998, 331, 659–668.
41. Liu, L.; Hausladen, A.; Zeng, M.; Que, L.; Heitman, J.; Stamler, J. S. Nature 2001, 410, 490–494.
42. Sanghani, P. C.; Bosron, W. F.; Hurley, T. D. Biochemistry 2002, 41, 15189–15194.
43. Tutino, M. L.; di Prisco, G.; Marino, G.; de Pascale, D. Protein Pept Lett 2009, 16, 1172–1180.
44. Laemmli, U. K. Nature 1970, 227, 680–685.
45. Uotila, L. Methods Enzymol 1981, 77, 426–428.
46. Bradford, M. M. Anal Biochem 1976, 72, 248–254.
47. Otwinowski, Z.; Minor, W. Methods Enzymol 1997, 276, 307–326.
48. Navaza, J. Acta Crystallogr Sect A 1994, 50, 157–163.
49. Jones, T. A.; Zou, J. Y.; Cowan, S. W.; Kjeldgaard, M. Acta Crystallogr Sect A 1991, 47, 110–119.

Reviewing Editor: Stephen Blacklow